Supplementary Information

Eetu Kari[1], Liqing Hao[1], Arttu Ylisirniö[1], Angela Buchholz[1], Ari Leskinen[1,2], Pasi Yli-Pirilä[3], Ilpo Nuutinen[3,a], Kari Kuuspalo[3,a], Jorma Jokiniemi[3], Celia L. Faiola[4,5], Siegfried Schobesberger[1], Annele Virtanen[1]

[1] Department of Applied Physics, University of Eastern Finland, Kuopio, Finland

[2] Finnish Meteorological Institute, Kuopio, Finland

[3] Department of Environmental and Biological Sciences, University of Eastern Finland, Kuopio, Finland

[4] Department of Ecology and Evolutionary Biology, University of California Irvine, Irvine, CA, United States

[5] Department of Chemistry, University of California Irvine, Irvine, CA, United States

[a] Currently working at Savonia University of Applied Sciences, Kuopio, Finland

Correspondence to: Annele Virtanen (annele.virtanen@uef.fi)

S1 Experimental procedure for Pure α-pin experiments

First, ammonium sulphate (AS) seed particles were fed into the chamber in an amount comparable to the primary particle mass loadings observed during vehicle exhaust experiments. Then, for Pure α-pin high NOx experiments, NO and NO_2 were introduced into the chamber so that NO_x concentration and NO_2-to-NO ratio were comparable to Mixed experiments. For Pure α-pin NOx free experiments, no NO_x was added. After that ~3 µl of butanol-d9 and ~1 µl (5 ppbv) of α-pinene were injected into the chamber. In high NOx experiments, propene was added before switching the BL-lamps on to adjust the VOC-to-NO_x ratio. Last, H_2O_2 was introduced into the chamber for OH-radical generation. After BL-lamps were switched on the photochemistry period was continued for 4 hours.

S2 Details from fragmentation of vehicle emitted aromatic VOCs inside the PTR-ToF-MS

With the PTR-MS technique, when H_3O^+ ions are used for ionization, separation of any isomeric compounds cannot be achieved. This causes problems in accounting for the degree of fragmentation, if information about the structure of the compounds is missing because some isomers go through higher fragmentation than others. Moreover, if the degree of fragmentation is not known or cannot be estimated, the quantification of measured compound is not possible without high uncertainties. For example, some aromatic compounds inside the drift tube of the PTR-ToF-MS undergo fragmentation while the others do not, even if they would have same elemental composition (Gueneron et al., 2015). Therefore, the degree of

fragmentation depends on the structure of the compound and the drift tube settings (mainly E/N value) (Gueneron et al., 2015;Kari et al., 2018).

Based on previous studies we can be sure that SOA precursors measured in this study from gasoline exhaust are mainly comprised of isomers of the compounds that do not go through substantial fragmentation inside the drift tube. For example, previous studies have identified the composition of gasoline exhaust showing that xylene isomers dominate over ethyl benzene detected at integer m/z 107, and trimethylbenzene isomers dominate over other isomers of C3-benzenes detected at integer m/z 121 (Schmitz et al., 2000;Schauer et al., 2002;Nordin et al., 2013;Platt et al., 2013;Gueneron et al., 2015). As the aromatic VOCs having only methyl substituents do not undergo fragmentation inside the PTR-ToF-MS, under the settings we operated the PTR-ToF-MS, we were able to quantitate them. Moreover, some of the detected oxygenated aromatics, such as benzaldehyde, do not go through substantial fragmentation inside the PTR-ToF-MS under the settings we operated the PTR-ToF-MS during the measurement campaign (Warneke et al., 2003;Maleknia et al., 2007;Schwarz et al., 2009). Therefore, for several SOA precursors measured with the PTR-ToF-MS we can be confident that substantial fragmentation inside the PTR-ToF-MS did not occur, and we were able to quantify these compounds without high uncertainties. However, we cannot assume that the fragmentation of all SOA precursors is unsubstantial, because we cannot identify their molecular structures or get information about the structure from literature that would enable us to estimate the degree of fragmentation they may undergo inside the drift tube. These species were mainly oxygenated aromatics, hence for these SOA precursors the calculated reacted concentrations may be incorrect that underestimates the predicted SOA mass from reactions between OH-radicals and these SOA precursors, while the fragmentation overestimates the concentration of benzene and toluene reported because the fragments of many larger aromatics possess their structural form in addition to small alkanes and alkenes present for example at mass integers m/z 41 and 43 (Gueneron et al., 2015).

S3 Linear combination analysis

GDI vehicle exhaust formed SOA during the photo-oxidation period in each experiment conducted during the measurement campaign. Hence, in Mixed experiments GDI vehicle derived SOA had to be subtracted from total SOA before α-pinene SOA mass yield was calculated. The estimations of GDI vehicle derived SOA in Mixed experiments causes uncertainty for the α-pinene SOA mass yield calculation. To decrease this uncertainty from our analysis, we did a linear combination analysis for all experiments where we assumed that without any other interactions than "NO_x effect" between anthropogenic and biogenic emissions the formed SOA in Mixed experiments would be equal to the sum of formed SOA in Pure Vehicle and Pure α-pin high NOx experiments, when the same amount of SOA precursors had reacted. The results of linear combination analysis are shown in Figure S5 that includes data points where each Pure α-pin High NOx experiment is summed up with each Pure Vehicle experiment (referred as Sum experiments). Figure S5 shows that when the same amount of SOA precursors has reacted, higher SOA formation is observed in Sum experiments compared to Mixed experiments. This shows that SOA

formation in Mixed experiments is not a linear combination from Pure Vehicle and Pure α-pin High NOx experiments. We want to highlight that the plotted "maximum SOA" for Mixed experiments is the measured SOA, i.e. we have not subtracted any fraction from total SOA to exclude the uncertainties that may have originated in the estimation of the formed gasoline vehicle derived SOA. The results shown in Figure S5 provide an additional piece of evidence that some other mechanism in addition to NO_x plays a role in the suppression of α-pinene SOA formation in the presence of gasoline vehicle exhaust. We observed that at minimum 20% more SOA was formed in Sum experiment (datapoint 11) compared to comparable Mixed experiment (datapoint 5). For this pair, the same amount of SOA precursors had reacted. As another pair we compared datapoint 6 (Mixed experiment) and datapoint 21 (Sum experiment). For this pair, 8% more SOA was formed in Sum experiment (datapoint 21) compared to Mixed experiment (datapoint 6) when 19% less SOA precursors had reacted in Sum experiment compared to Mixed experiment.

The linear combination analysis demonstrates that NO_x present in Mixed experiments cannot alone explain the observed decrease in SOA formation, because both NO and NO_2 concentrations were comparable between all experiments (see Table 2). Moreover, based on the GDI vehicle included experiments, we can conclude that the differences in GDI vehicle emitted IVOC and SVOC SOA precursors cannot explain this high discrepancies in formed SOA between Mixed and Sum experiments either. This is because same VOC SOA precursors, with varying concentrations depending on the feeding time, were introduced into the chamber in each experiment. Moreover, similar concentrations of THC were measured with the FTIR from raw undiluted exhaust in each experiment. Therefore, even if we were not able to measure IVOCs and SVOCs during this campaign, we can be confident that in Mixed experiments GDI vehicle emitted SOA forming SVOCs and IVOCs were quantitatively and qualitatively comparable with the species emitted during Pure Vehicle experiments.

References

Chan, A. W. H., Kautzman, K. E., Chhabra, P. S., Surratt, J. D., Chan, M. N., Crounse, J. D., Kurten, A., Wennberg, P. O., Flagan, R. C., and Seinfeld, J. H.: Secondary organic aerosol formation from photooxidation of naphthalene and alkylnaphthalenes: implications for oxidation of intermediate volatility organic compounds (IVOCs), Atmos Chem Phys, 9, 3049-3060, 10.5194/acp-9-3049-2009, 2009.

Chhabra, P. S., Flagan, R. C., and Seinfeld, J. H.: Elemental analysis of chamber organic aerosol using an aerodyne high-resolution aerosol mass spectrometer, Atmos Chem Phys, 10, 4111-4131, 10.5194/acp-10-4111-2010, 2010.

Chhabra, P. S., Ng, N. L., Canagaratna, M. R., Corrigan, A. L., Russell, L. M., Worsnop, D. R., Flagan, R. C., and Seinfeld, J. H.: Elemental composition and oxidation of chamber organic aerosol, Atmos Chem Phys, 11, 8827-8845, 10.5194/acp-11-8827-2011, 2011.

Gueneron, M., Erickson, M. H., VanderSchelden, G. S., and Jobson, B. T.: PTR-MS fragmentation patterns of gasoline hydrocarbons, Int J Mass Spectrom, 379, 97-109, 10.1016/j.ijms.2015.01.001, 2015.

Hildebrandt, L., Donahue, N. M., and Pandis, S. N.: High formation of secondary organic aerosol from the photo-oxidation of toluene, Atmos Chem Phys, 9, 2973-2986, DOI 10.5194/acp-9-2973-2009, 2009.

Kari, E., Miettinen, P., Yli-Pirila, P., Virtanen, A., and Faiola, C. L.: PTR-ToF-MS product ion distributions and humidity-dependence of biogenic volatile organic compounds, Int J Mass Spectrom, 430, 87-97, 10.1016/j.ijms.2018.05.003, 2018.

Li, L. J., Tang, P., Nakao, S., and Cocker, D. R.: Impact of molecular structure on secondary organic aerosol formation from aromatic hydrocarbon photooxidation under low-NOx conditions, Atmos Chem Phys, 16, 10793-10808, 10.5194/acp-16-10793-2016, 2016.

Maleknia, S. D., Bell, T. L., and Adams, M. A.: PTR-MS analysis of reference and plant-emitted volatile organic compounds, Int J Mass Spectrom, 262, 203-210, 10.1016/j.ijms.2006.11.010, 2007.

Ng, N. L., Kroll, J. H., Chan, A. W. H., Chhabra, P. S., Flagan, R. C., and Seinfeld, J. H.: Secondary organic aerosol formation from m-xylene, toluene, and benzene, Atmos Chem Phys, 7, 3909-3922, DOI 10.5194/acp-7-3909-2007, 2007.

Nordin, E. Z., Eriksson, A. C., Roldin, P., Nilsson, P. T., Carlsson, J. E., Kajos, M. K., Hellen, H., Wittbom, C., Rissler, J., Londahl, J., Swietlicki, E., Svenningsson, B., Bohgard, M., Kulmala, M., Hallquist, M., and Pagels, J. H.: Secondary organic aerosol formation from idling gasoline passenger vehicle emissions investigated in a smog chamber, Atmos Chem Phys, 13, 6101-6116, 10.5194/acp-13-6101-2013, 2013.

Platt, S. M., El Haddad, I., Zardini, A. A., Clairotte, M., Astorga, C., Wolf, R., Slowik, J. G., Temime-Roussel, B., Marchand, N., Jezek, I., Drinovec, L., Mocnik, G., Mohler, O., Richter, R., Barmet, P., Bianchi, F., Baltensperger, U., and Prevot, A. S. H.: Secondary organic aerosol formation from gasoline vehicle emissions in a new mobile environmental reaction chamber, Atmos Chem Phys, 13, 9141-9158, 10.5194/acp-13-9141-2013, 2013.

Schauer, J. J., Kleeman, M. J., Cass, G. R., and Simoneit, B. R. T.: Measurement of emissions from air pollution sources. 5. C-1-C-32 organic compounds from gasoline-powered motor vehicles, Environ Sci Technol, 36, 1169-1180, 10.1021/es0108077, 2002.

Schmitz, T., Hassel, D., and Weber, F. J.: Determination of VOC-components in the exhaust of gasoline and diesel passenger cars, Atmos Environ, 34, 4639-4647, Doi 10.1016/S1352-2310(00)00303-4, 2000.

Schwarz, K., Filipiak, W., and Amann, A.: Determining concentration patterns of volatile compounds in exhaled breath by PTR-MS, J Breath Res, 3, Artn 02700210.1088/1752-7155/3/2/027002, 2009.

Warneke, C., De Gouw, J. A., Kuster, W. C., Goldan, P. D., and Fall, R.: Validation of atmospheric VOC measurements by proton-transfer-reaction mass spectrometry using a gas-chromatographic preseparation method, Environ Sci Technol, 37, 2494-2501, 10.1021/es026266i, 2003.

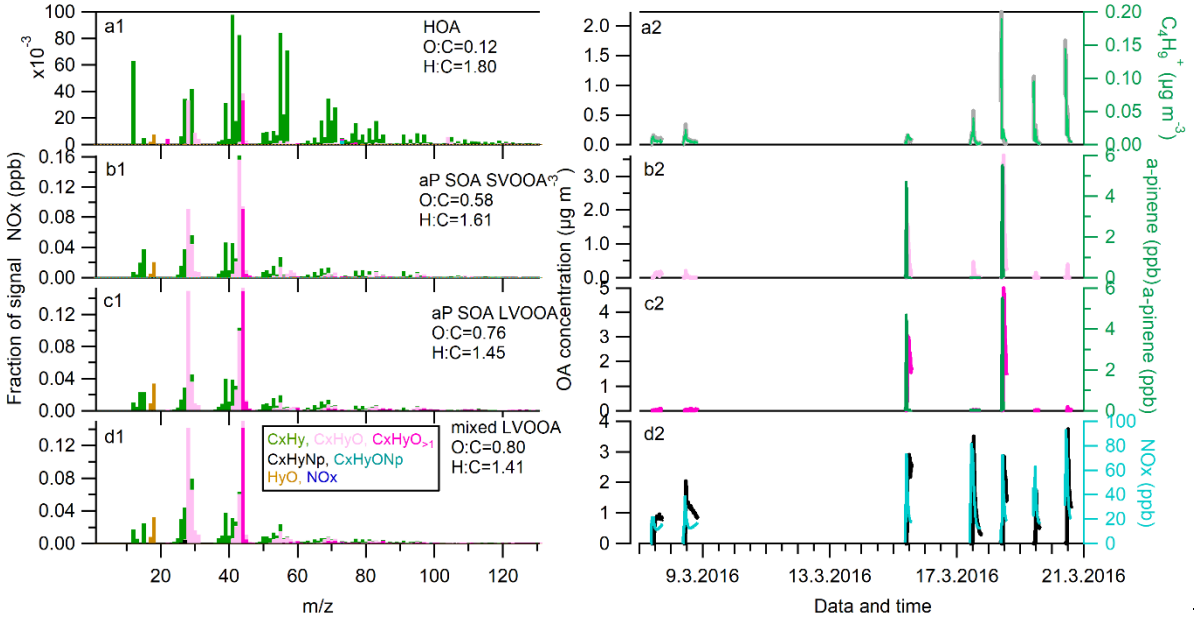

Figure S1. PMF factor solutions to the high-resolution mass spectra: profiles (left panels) and time series (right panels). Tracers were selected to correlate with the factor time series.

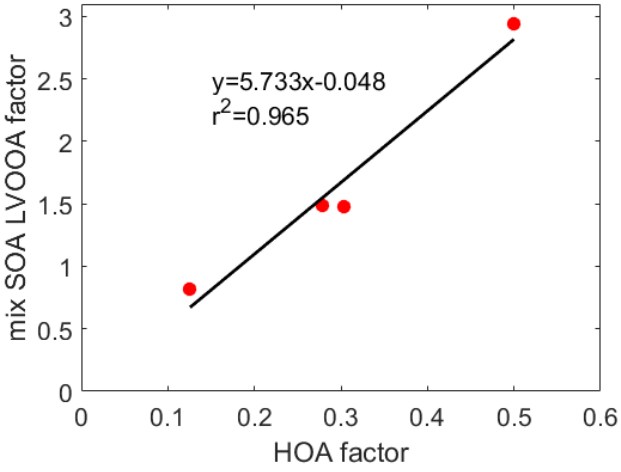

Figure S2. HOA factor as a function of mix_SOA_LVOOA factor in Pure Vehicle experiments.

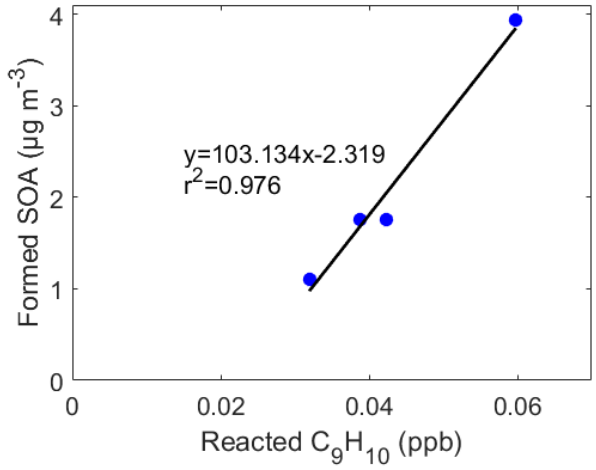

Figure S3. Reacted concentration of C_9H_{10} as a function of formed SOA in Pure Vehicle experiments.

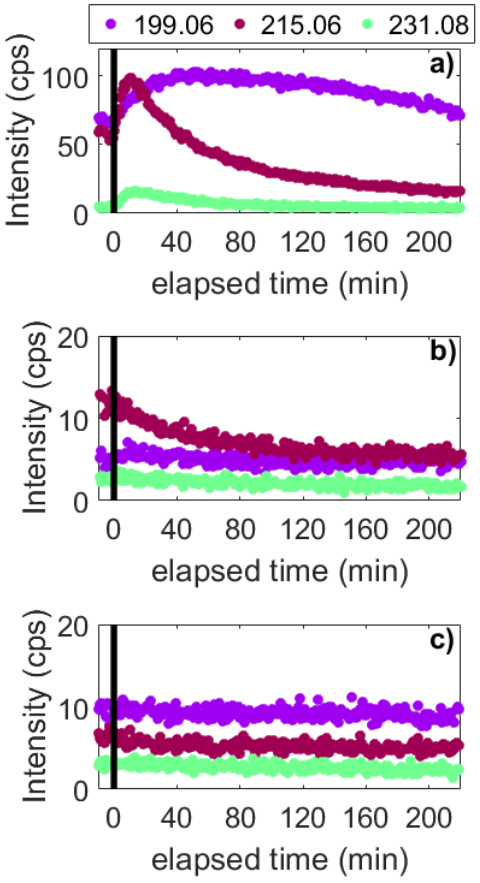

Figure S4. Temporal evolution of acetate-ToF-CIMS measured oxidation products formed when α-pinene and gasoline vehicle exhaust were both present in the chamber during the photochemistry (panel a)). Panels b) and c) show the evolution of same compounds during Pure Vehicle and Pure α-pin high NOx experiments to demonstrate the absence of these compounds when only α-pinene or gasoline vehicle exhaust were present inside the chamber during the photochemistry period. At time zero the photochemistry experiment was started when BL lamps were switched on.

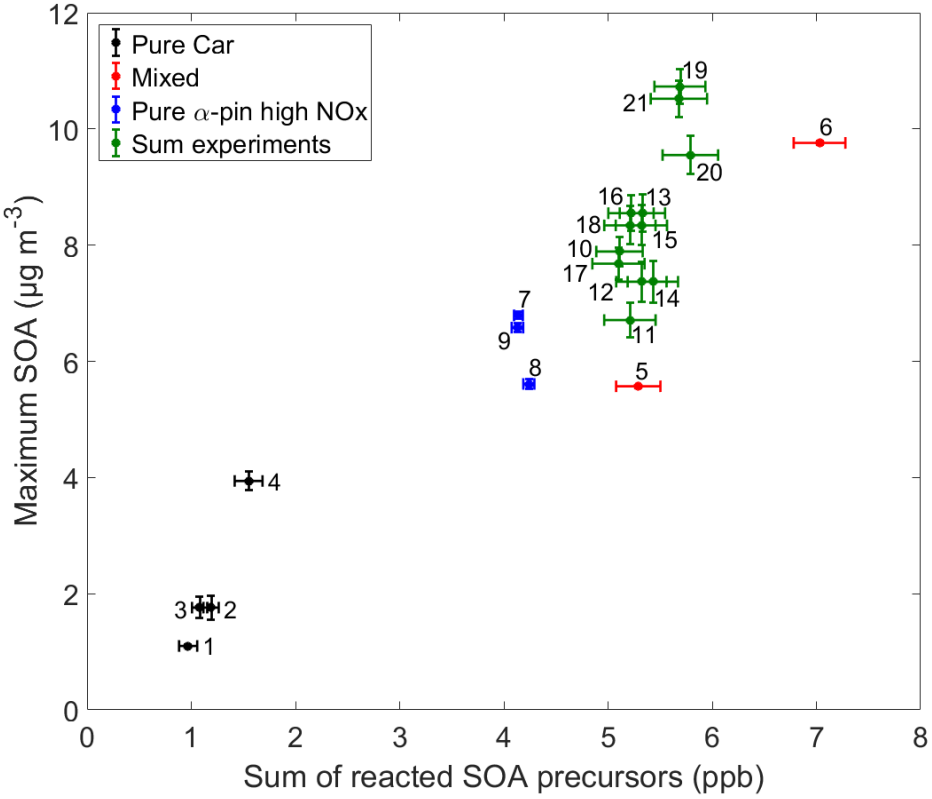

Figure S5. Maximum SOA as a function sum of reacted SOA precursors for all experiments including so-called "Sum experiments" where the SOA mass obtained from each Pure Vehicle experiment has been summed with that from each Pure α-pin High NOx experiment. Error bars for the x-axis are estimated from uncertainties in PTR-ToF-MS measurements (one standard deviation of 10 min averaged datapoints of each VOC), and total error for the x-axis was calculated using a propagation of uncertainty when Sum of reacted SOA precursors (x-axis) included the reacted mass concentrations of α-pinene and aromatic VOCs listed in Table S2 or just aromatic VOCs. Error bars for the y-axis are estimated from uncertainties in SP-AMS measurements (one standard deviation of 20 min averaged datapoints). For Sum experiments errors were calculated using a propagation of uncertainty for PTR-ToF-MS (x-axis errors) and AMS (y-axis errors) uncertainties.

Table S1. Organic compounds calibrated for FTIR that were used to calculate THC values from the raw exhaust.

Gas	Formula	Range	Unit
Methane	CH4	1000	ppm
Ethane	C2H6	200	ppm
Propane	C3H8	200	ppm
Butane	C4H10	200	ppm
Pentane	C5H12	200	ppm
Hexane	C6H14	200	ppm
Heptane	C7H16	200	ppm
Octane	C8H18	200	ppm
Acetylene	C2H2	200	ppm
Ethylene	C2H4	200	ppm
Propene	C3H6	200	ppm
1,3-Butadiene	C4H6	200	ppm
Benzene	C6H6	200	ppm
Toluene	C7H8	200	ppm
m-Xylene	C8H10	200	ppm
o-Xylene	C8H10	200	ppm
p-Xylene	C8H10	200	ppm
1,2,3-Trimethylbenzene	C9H12	200	ppm
1,2,4-Trimethylbenzene	C9H12	200	ppm
1,3,5-Trimethylbenzene	C9H12	200	ppm
Formic acid	CH2O2	200	ppm
Acetic acid	C2H4O2	200	ppm
Formaldehyde	CH2O	200	ppm
Acetaldehyde	C2H4O	200	ppm

Table S1 continues. Organic compounds calibrated for FTIR that were used to calculate THC values from the raw exhaust.

Gas	Formula	Range	Unit
Methanol	CH3OH	500	ppm
Ethanol	C2H5OH	500	ppm
Propanol	C3H7OH	500	ppm
Methyl tertiary butyl ether	C5H12O	200	ppm

Table S2. SOA precursors applied for predicted SOA calculation.

Suggested name[1]	Formula	SOA mass Yield Lower estimate	SOA mass Yield Higher estimate	References for SOA mass yields and possible proxy for yield
Benzene	C6H6	0.156	0.281	(Ng et al., 2007)
Toluene	C7H8	0.08	0.32	(Ng et al., 2007;Hildebrandt et al., 2009)
Phenol	C6H6O	0.34	0.34	(Chhabra et al., 2011)
Styrene	C8H8	0.035	0.059	(Ng et al., 2007), Xylene
Benzaldehyde	C7H6O	0.08	0.32	(Ng et al., 2007), Toluene
Xylene	C8H10	0.035	0.059	(Ng et al., 2007)
C9-aromatic	C9H8	0.049	0.065	(Li et al., 2016), Trimethylbenzene
C9-aromatic	C9H10	0.049	0.065	(Li et al., 2016), Trimethylbenzene
Methyl-benzaldehyde	C8H8O	0.08	0.32	(Ng et al., 2007), Toluene
Trimethylbenzene	C9H12	0.049	0.065	(Li et al., 2016)
Naphtalene	C10H8	0.2	0.222	(Chan et al., 2009;Chhabra et al., 2010)
C10-aromatic	C10H12	0.049	0.065	(Li et al., 2016), Trimethylbenzene
Oxygen containing C8-aromatic	C8H6O2	0.111	0.111	(Chhabra et al., 2011), Syringol
Oxygen containing C9-aromatic	C9H10O	0.111	0.111	(Chhabra et al., 2011), Syringol
C10-aromatic	C10H14	0.049	0.065	(Li et al., 2016), Trimethylbenzene
C11-aromatic	C11H14	0.2	0.222	(Chan et al., 2009;Chhabra et al., 2010), Naphtalene
Oxygen containing C10-aromatic	C10H12O	0.111	0.111	(Chhabra et al., 2011), Syringol
C11-aromatic	C11H16	0.049	0.065	(Li et al., 2016), Trimethylbenzene
C12-aromatic	C12H18	0.049	0.065	(Li et al., 2016), Trimethylbenzene
Oxygen containing C10-aromatic	C10H12O2	0.111	0.111	(Chhabra et al., 2011), Syringol

[1] Suggested name is based on the identified molecular structure and literature